ELSEVIER

Ceramics International 30 (2004) 643–652

CERAMICS INTERNATIONAL

www.elsevier.com/locate/ceramint

Sintering characteristics of talc in the presence of phosphatic and alkali carbonate sintering activators

Navin Chandra*, Nitin Agnihotri, Sanjeev Kumar Bhasin

Regional Research Laboratory (CSIR), Habibganj Naka, Hoshangabad Road, Bhopal-462 026 (M.P.), India

Received 8 November 2002; received in revised form 24 April 2003; accepted 28 August 2003

Available online 17 March 2004

Abstract

The sintering characteristics of three-layer monoclinic natural talc sample occurring in Jabalpur District of Madhya Pradesh (India) have been investigated in the presence of sintering activators. The mineral is observed to undergo dehydroxylation reaction on heat treatment. The dehydroxylation reaction occurs at a lower temperature in the presence of added activator of sintering.

The dehydroxylate species react with sodium carbonate to form $Na_2Si_2O_5$ and Na_2MgSiO_4 phases leading to mechanical strength in the sintered body. In the case of phosphatic species (H_3PO_4/sodium hexametaphosphate (SHMP)) added to serve as activators of sintering, $Mg_3(PO_4)_2$/$Mg(PO_3)_2$/$NaMgPO_4$ phases are formed. The impact strength of the tile-shaped samples made in the presence of phosphoric acid is observed to be higher than that of those made with only sodium carbonate. The impact strength of samples is observed to increase with increase in SHMP content. The SEM micrographs show the formation of fairly large size crystals when talc is sintered with H_3PO_4. In the case of other activators of sintering (viz. Na_2CO_3 and SHMP), significant amount of smaller crystals are also observed to be present.

Keywords: Sintering; Activator of sintering; Sodium hexametaphosphate (SHMP); Talc

1. Introduction

Talc is a three-layered clay mineral of the pyrophyllite group [1–3], having chemical formula $Mg_3Si_4O_{10}(OH)_2$. Its structure comprises of a magnesium–oxygen–hydroxyl octahedral brucite layer, sandwiched between two sheets of silicon–oxygen tetrahedral. The adjacent layers are held together by weak van der Waals forces and hence give rise to a soapy feeling in the talc [1–3].

The reserves of talc in India are estimated to be 83.66 million tons [4]. In 1998–1999 its production in India was reported to be 0.643 million tons [5]. In the same year, the main talc producing countries, namely, China, USA, Finland, India, France and Brazil, produced 4.354 million tons while other smaller producers accounted for a production of 2.946 million tons of talc [5].

Talc is a high melting point (1500 °C), hydrophobic, non-polar, organophilic material [3] and is widely used in cosmetics, paper, rubber, paints [6] and food industries [7] as an additive due to its comparatively low cost. It is a ceramic/refractory material and is extensively used for making wall tiles, electrical insulators, ceramic porcelain, kiln furniture, etc. [8]. Due to its electrical and thermal properties, talc is an attractive material for engineering applications [9]. However, its wider use for such applications has been hindered due to lack of systematic studies on its processing characteristics, specially in the presence of non-conventional sintering additives and activators. In the present paper, we report the results of our studies on the sintering characteristics of talc in the presence of sodium carbonate and phosphate-based sintering activators.

2. Experimental

2.1. Chemicals

Lumps of talc mineral, collected from mines in Jabalpur District of M.P. were used in the present study. The lumps were crushed manually and then powdered using a ball mill. The sieve analysis of the sample showed that 1.8% of the sample was of +400 μm, 90.2% was in the range −400 to

* Corresponding author. Tel.: +91-755-2782360; fax: +91-755-2587042/2488323.
E-mail address: navinchandrarrl@yahoo.com (N. Chandra).

0272-8842/$30.00
doi:10.1016/j.ceramint.2003.08.007

+150 μm, 7.9% was in the range −150 to +75 μm and 0.1% was of −75 μm size.

A.R. grade Ranbaxy make phosphoric acid and L.R. grade sodium hexametaphosphate (SHMP) and sodium carbonate of S.D. Fine Chemical make were used.

2.2. Chemical analysis of talc

Standard methods of wet chemical analysis [10] were used for the determination of silica and alumina. The content of magnesium, iron and calcium was determined using inductively coupled plasma spectrometer (Jobin Yvon, Model: JY-2000). The content of sodium and potassium was determined using Systronics make flame photometer (Model: Mediflame).

2.3. X-ray diffraction studies

For identification of the crystallized phases present in the talc sample (with and without heat treatment) as well as in the sintered bodies, Philips X-ray diffractometer (Model No. 1710) was used. The measurements were made at 30 mA current and 40 kV accelerating voltage using Ni-filtered Cu kα radiation in the 5–75° 2θ ranges. The identification of the phases was carried out by comparing the experimentally observed inter planar spacing ("*d*" values) and the intensity of the peaks with the *d* values of the respective likely substances/phases given in the Mineral Powder Diffraction Search Manual [11].

2.4. Thermal analysis

The thermal behavior of talc sample and talc+10% SHMP composition was studied using Lenseis make simultaneous thermal analyzer (Model L-81) in the temperature range ambient to 1200 °C at a heating rate of 10 °C/min.

2.5. Impact strength of sintered bodies

The impact strength of the sintered bodies made from talc + SHMP, talc + Na_2CO_3, talc + H_3PO_4 and talc + H_3PO_4 + Na_2CO_3 compositions was determined following the procedure laid down in the IS Specifications [12]. The samples required for these studies were prepared by thorough mixing of the talc and SHMP in required proportion (moisture content 4%) followed by compression of about 100 g mixture in a 10 cm × 10 cm bed size steel mould at 1.50×10^6 kg/m^2 pressure to obtain tile-like samples of about 4 mm thickness following the procedure published earlier [13,14]. The compressed samples were dried in an air oven at 110 °C for 3 h followed by sintering in an electrical furnace at 950 °C for 1 h. The samples were allowed to cool in the furnace to ambient temperature.

2.6. Porosity and density measurements

The porosity of sintered bodies was determined by water absorption measurements following the procedure laid down in IS Specifications [12]. The apparent density of the green and sintered tile samples was determined by exactly measuring their weight and dimensions.

2.7. Scanning electron microscopic studies

Scanning electron microscope (Jeol Model: JSM 5600) was used to study the morphology of talc samples (with and without heat treatment at 950 °C) and of sintered talc + SHMP (10%, w/w), talc + H_3PO_4 (10%, w/w), talc + Na_2CO_3 (10%, w/w) and talc + 10% H_3PO_4 + 10% Na_2CO_3 after powdering using mortar and pestle. The micrographs are given in Figs. 5–10.

3. Results

The results of the chemical analysis of the talc sample used in the present study are given in Table 1. As expected from the chemical formula of the mineral ($Mg_3Si_4O_{10}(OH)_2$), the content of equivalent silica (60.35%) and MgO (29.20%) in the sample is high (theoretical values 63.3 and 31.9%, respectively). The loss on ignition in the sample is observed to be 4.02% as compared to theoretically expected value of 4.8%. Further, the content of calcium, iron and aluminium in the sample used is observed to be low, indicating that the sample is not substantially contaminated by dolomite, chlorite, calcite or clay materials, etc., which are generally associated with this mineral [6], and is fairly pure talc.

3.1. X-ray diffraction studies

3.1.1. X-ray diffraction of talc with and without heat treatment

The X-ray diffractograms of the talc sample, with and without heat treatment at 950 °C for 3 h, are shown in Fig. 1. The main peaks observed in the diffractogram of talc (cf. Fig. 1) have *d* values 9.34, 4.66, 3.11, 2.33, 1.87, 1.56,

Table 1
Chemical composition of talc mineral

Constituents	Theoretical value (%)	Experimentally observed value (%)
SiO_2	63.3	60.35
Fe_2O_3	–	0.22
Al_2O_3	–	1.86
MgO	31.9	29.20
CaO	–	0.12
Na_2O	–	1.20
K_2O	–	0.80
LOI	4.8	4.02

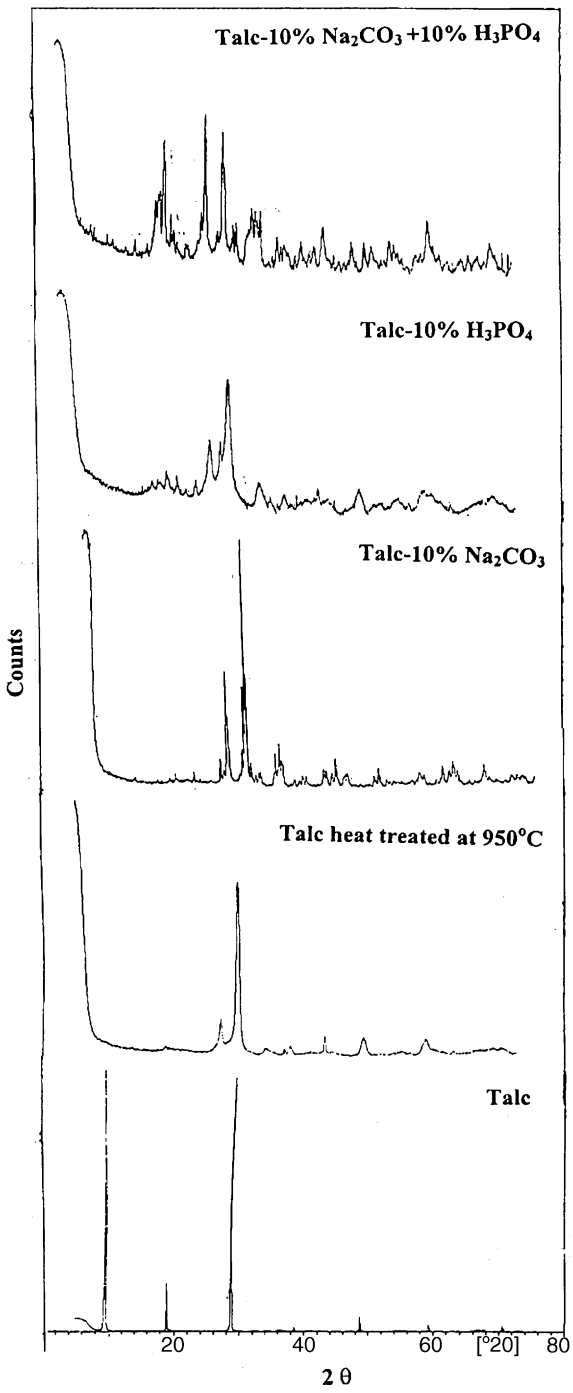

Fig. 1. X-ray diffraction patterns of talc and talc (heat treated at 950 °C) and talc sintered at 950 °C for 1 h in the presence of—10% Na_2CO_3, talc + 10% H_3PO_4 and talc + 10% H_3PO_4 + 10% Na_2CO_3.

1.39, 1.33 corresponding to talc [11]. The lattice constants, *a*, *b* and *c* were calculated corresponding to the observed "*d*" values and were observed to be 5.15, 9.29 and 18.89, respectively. From these values it is concluded that the talc used in the present studies is tri-layer monoclinic form of the mineral. On heat treatment at 950 °C for 3 h, talc sample is observed to undergo dehydroxylation reaction to form $MgSiO_3$ (enstatite) phase having "*d*" values 3.16, 2.86 and 2.52 (cf. Fig. 1), similar to the observations reported by Santos and Yada [15] and Mukherji et al. [8].

3.1.2. *X-ray diffraction of talc sintered in the presence of sintering activators*

The X-ray diffractograms of talc sintered at 950 °C in the presence of (i) 10% Na_2CO_3, (ii) 10% H_3PO_4 and (iii) 10% Na_2CO_3 + 10% H_3PO_4 are shown in Fig. 1 and those for 7, 8, 9 and 10% SHMP are shown in Fig. 2. The *d* values of the phases formed on sintering are listed in Table 2. Enstatite ($MgSiO_3$) is observed to be present in all the sintered samples and silica is formed when phosphate ion is present in the sintering additive.

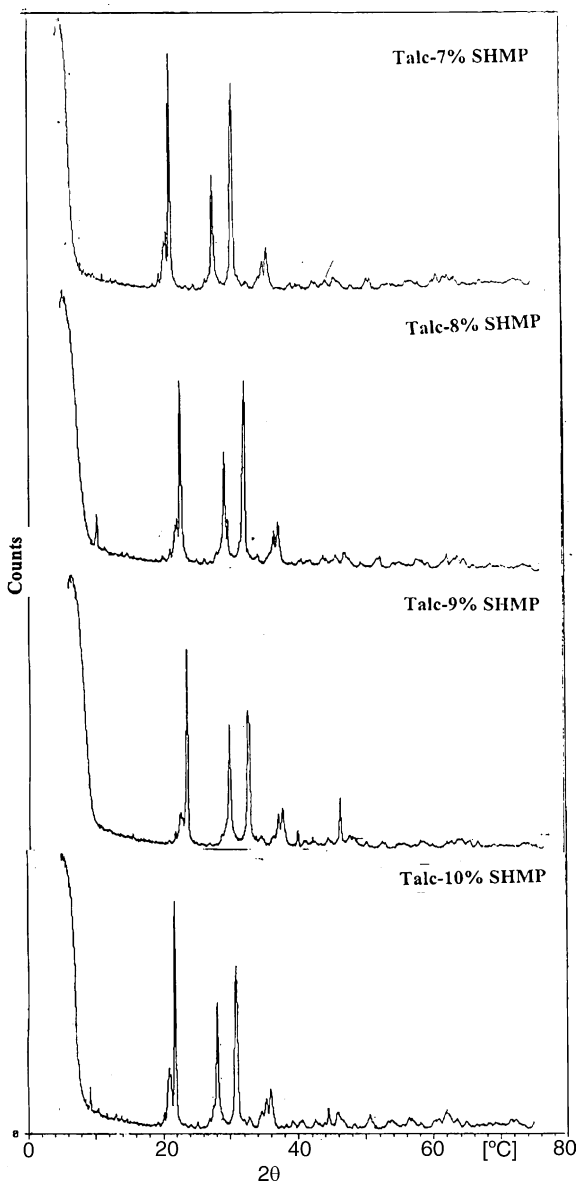

Fig. 2. X-ray diffraction patterns of talc sintered at 950 °C for 1 h in the presence of—7, 8, 9 and 10% sodium hexametaphosphate.

Table 2
Phases formed on sintering of talc in the presence of different sintering activators

Name of observed phase	Talc + 10% Na_2CO_3 mix	Talc + 10% H_3PO_4 mix	Talc + 10% H_3PO_4 + 10% Na_2CO_3 mix	Talc + SHMP mix
$MgSiO_3$ (Enstatite)	3.16, 2.86 and 2.52	2.86, 3.16 and 2.52	2.86, 3.15 and 2.51	2.86, 3.16 and 2.52
Silica (SiO_2)	Absent	4.05, 2.50, 2.86, 2.43 and 2.01	4.05, 2.49, 2.43, 2.11, 2.01 and 1.43.	4.05, 2.86, 2.49, 2.11 and 2.03
Mg_2SiO_4	2.48, 2.26 and 3.86	2.48, 2.26 and 3.86	Absent	2.48, 2.52, 2.27, 1.78 and 1.48
β-Mg_2SiO_4	Absent	Absent	Absent	2.03, 2.49 and 2.21
$Na_2Si_2O_5$	3.23 and 2.93	Absent	4.21, 2.94, 3.25, 2.30	4.21, 3.28 and 2.59
Na_2MgSiO_4	2.59, 2.11, 1.81, 1.50 and 1.41.	Absent	2.59, 4.21, 1.49, 1.83, 2.11	4.21, 2.11, 1.50 and 1.41
$Mg(PO_3)_2$	Absent	2.99 and 4.56	2.99, 4.56, 3.23	Absent
$Mg_3(PO_4)_2$	Absent	3.42, 3.83 and 2.40	Absent	Absent
$NaMgPO_4$ (α, γ and ε forms)	Absent	Absent	3.80, 3.70, 2.75, 2.70, 2.55, 2.15, 2.24, 1.84 and 1.71	2.70, 2.55, 2.21, 1.84 and 1.72

"*d*" values of observed phases in X-ray diffraction pattern of sintered talc with different sintering activators.

3.1.3. Thermal analysis

The DTA and TGA curves for the talc sample are shown in Fig. 3. Initially, as the temperature increases from the ambient, an exothermic effect with a peak at 90 °C, and accompanied by a 0.53% weight gain (cf. TG curve), is observed. A similar observation of gain in weight has been reported earlier and has been attributed to the oxidation of the impurity phases [16] in this temperature region. As the temperature is further increased, the TG curve remains almost flat in the temperature range 90–860 °C. However, the DTA curve shows a broad exothermic effect in the range 130–300 °C. Between 860 and 1080 °C, a prominent endothermic effect is observed with a peak at 950 °C. This effect is accompanied by a significant weight loss of 3.97% (cf. TGA curve) and may be attributed to the slow dehydroxylation of the talc sample by removal of water from –OH

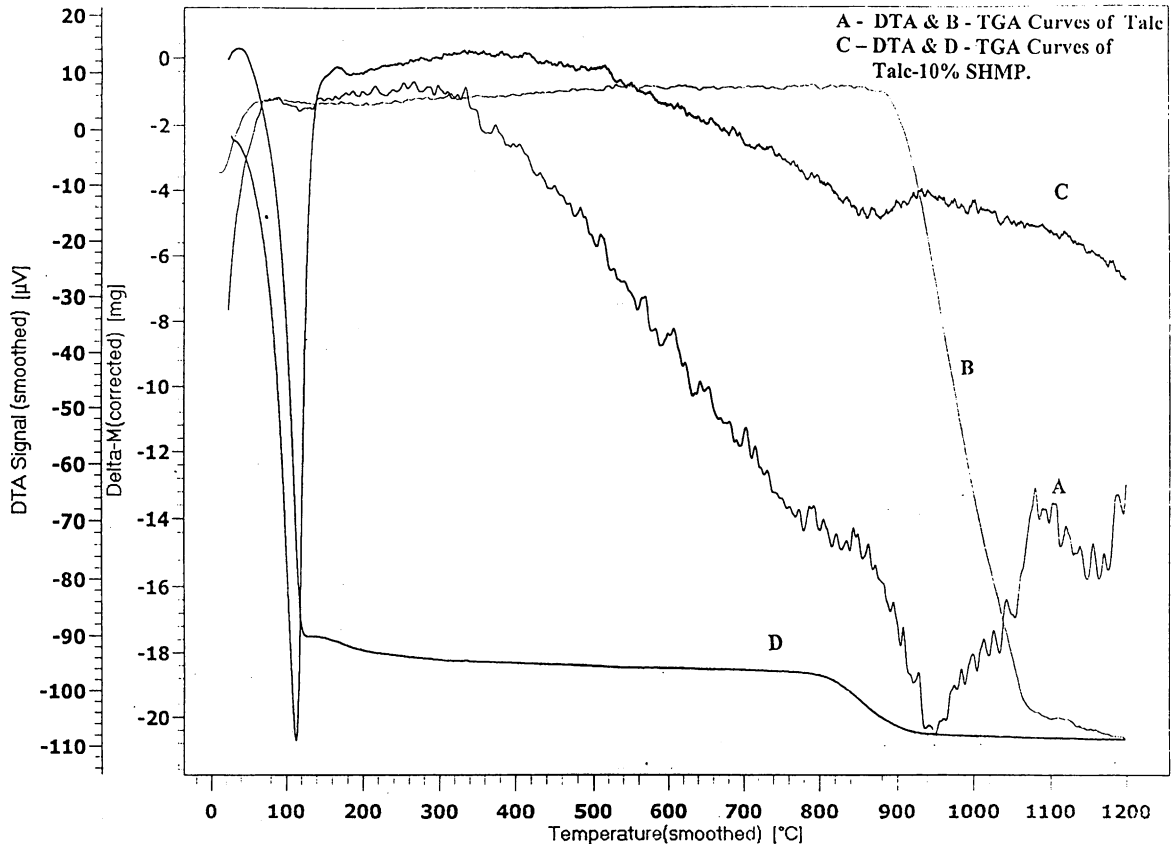

Fig. 3. DTA–TGA curves of talc and talc + 10% SHMP.

groups attached to Mg–O–OH layer and formation of magnesium silicate phases (mainly enstatite phase). The formation of enstatite on heating of talc has also been reported by Santos and Yada in this temperature range [16]. Between 1080 and 1200 °C, another endothermic effect with peak at 1160 °C is observed and may be attributed to the formation of silica (cristobalite) phase. The minor weight loss (0.22%) in the 1080–1200 °C temperature range may be attributed to a simultaneous dehydroxylation of still remaining hydroxyl species. The DTA and TGA curves for talc—SHMP mix (containing 10% SHMP) are also given in Fig. 3. The sample was prepared by dissolving exact quantity of SHMP in water and then thoroughly mixing the solution with required quantity of talc. The DTA of this mix shows a sharp endothermic peak at 110 °C corresponding to the vaporization of water and corresponds to about 32% water loss in TGA. With a further increase in temperature, a broad exothermic effect in the temperature range 130–540 °C, with a peak at 370 °C is observed. This is followed by an endothermic effect in the temperature range 780–940 °C with a peak at 850 °C and is accompanied by 3.5% weight loss and may be attributed to the formation of magnesium silicates (mainly enstatite) by dehydoxylation of talc and simultaneous reaction with SHMP by topotactic mechanism. It is notable here that in the sample containing SHMP, the dehydroxylation phenomenon sets in at a lower temperature of 780 °C as compared to 860 °C in talc sample and the peak is also shifted to a lower temperature of 850 °C as compared to 950 °C observed in talc sample. It has been shown that sodium as well as phosphate ions are highly effective activators for reducing the temperature of formation of different phases and sintering of pyrophyllite-based ceramic bodies [14,17–19]. The shift in the dehydroxylation of talc at lower temperature observed in the present case indicates that sodium SHMP serves as an activator for reduction of temperature of dehydroxylation of talc.

Table 3
The impact strength values for the samples made from talc-SHMP mix (containing 7, 8, 9 and 10% (w/w) SHMP)

S. no.	Composition of talc + activator	Impact strength (J/m^2)
1	10% sodium carbonate	2.96
2	10% phosphoric acid	4.54
3	10% phosphoric acid + 10% sodium carbonate	4.53
4	7% binder SHMP	2.43
5	8% binder SHMP	2.83
6	9% binder SHMP	3.34
7	10% binder SHMP	4.00

3.1.4. Impact strength of samples made from talc–SHMP mix

The impact strength values for the samples made from talc–SHMP mix (containing 7, 8, 9 and 10% (w/w) SHMP) are given in Table 3. It is observed that the impact strength of the talc body sintered with 7% SHMP is lowest and increases with increase in SHMP content. The impact strength of samples made using 10% H_3PO_4 (with or without 10% Na_2CO_3) is observed to be highest.

3.1.5. Apparent density and porosity

The plots of % water absorption and apparent density of sintered tile samples versus their composition are given in Fig. 4. The apparent density is observed to very marginally decrease with increase in the SHMP content in the composition and the apparent density of the compositions containing 10% Na_2CO_3, 10% H_3PO_4 and 10% Na_2CO_3 + 10%

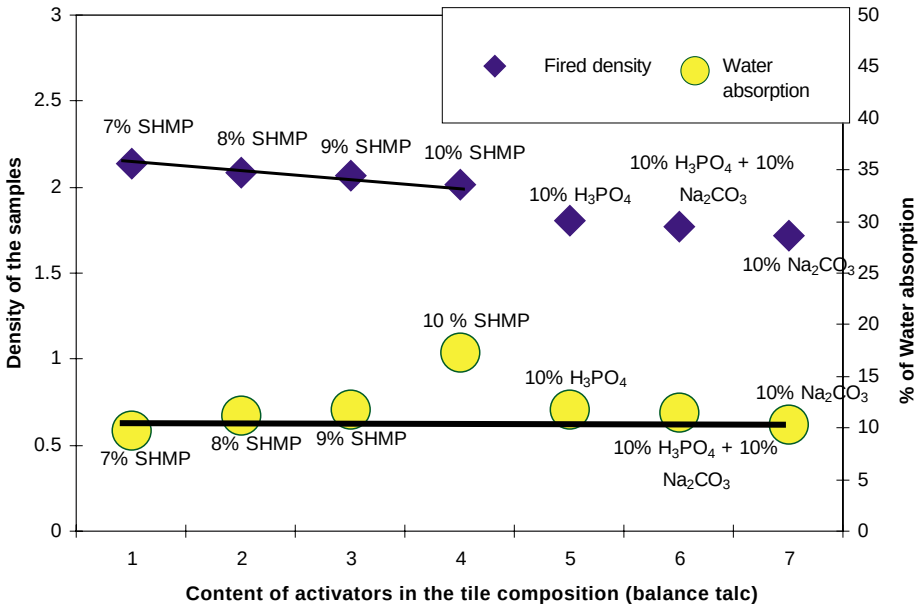

Fig. 4. Plot of fired density and % of water absorption vs. content of activators in the tile compositions.

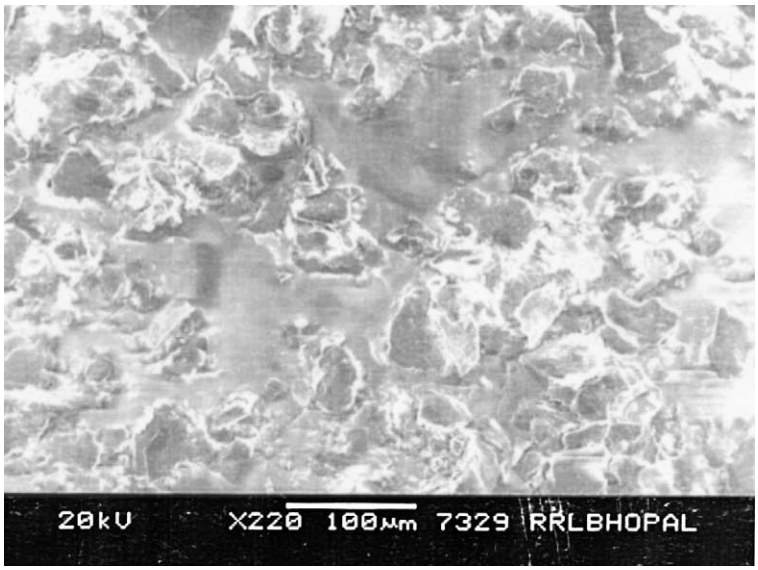

Fig. 5. SEM micrograph of talc.

H_3PO_4 is observed to be lower than those containing SHMP. As discussed earlier in this paper, the increase in the content of sintering activator lowers the temperature of dehydroxylation of talc. The TG curve has shown that on complete dehydroxylation, the talc sample releases 3.97% water. The minor decrease in the apparent density of the tile samples with increase in the content of activators may be attributed to the decrease in the weight due to loss of water from talc, which increases with the concentration of the activators. The % water absorption, indicating porosity in the samples is, however, observed to remain almost constant (~11%, w/w) at all the compositions studied. It appears that the % water absorption measurements are not sensitive enough to reflect the effect of minor changes in apparent density/porosity in the present samples.

3.1.6. Scanning electron microscopy

The SEM micrograph for powdered talc sample (cf. Fig. 5) shows the particles to be flaky in nature. On heat treatment at 950 °C for 1 h, the flakes are substantially converted to smaller size particles of irregular shape due to dehydroxylation leading to enstatite formation (cf. Fig. 6). On sintering of talc with 10% H_3PO_4 (w/w), a large number of fairly large size (30–50 μm) crystals together with smaller size (10–25 μm) crystals are seen to be formed (Fig. 7). However, when the talc is sintered in the presence of 10% Na_2CO_3 (either with (Fig. 8) or without (Fig. 10) 10% H_3PO_4), the crystal size is observed to decrease (10–30 μm) with some of the particles being even below 5 μm size. In the case of addition of 10% SHMP, the crystals are observed to be a mixture of small (5–10 μm) and

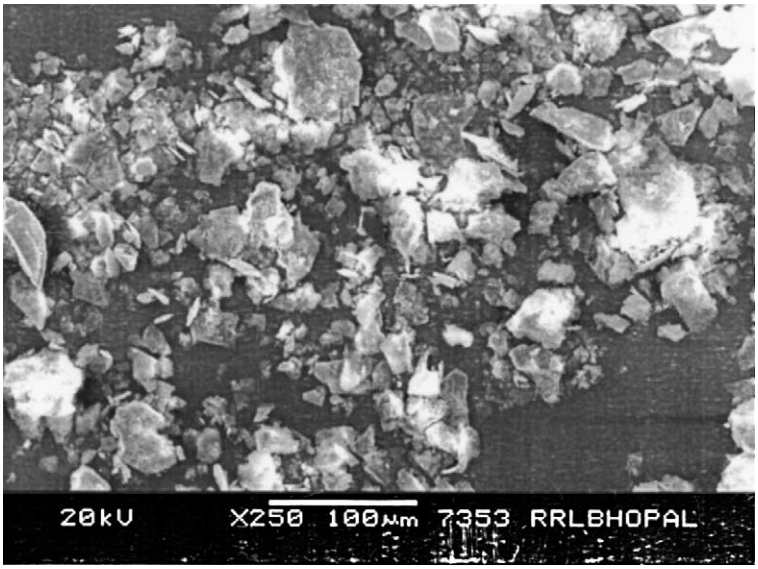

Fig. 6. SEM micrograph of talc (heat treated at 950 °C).

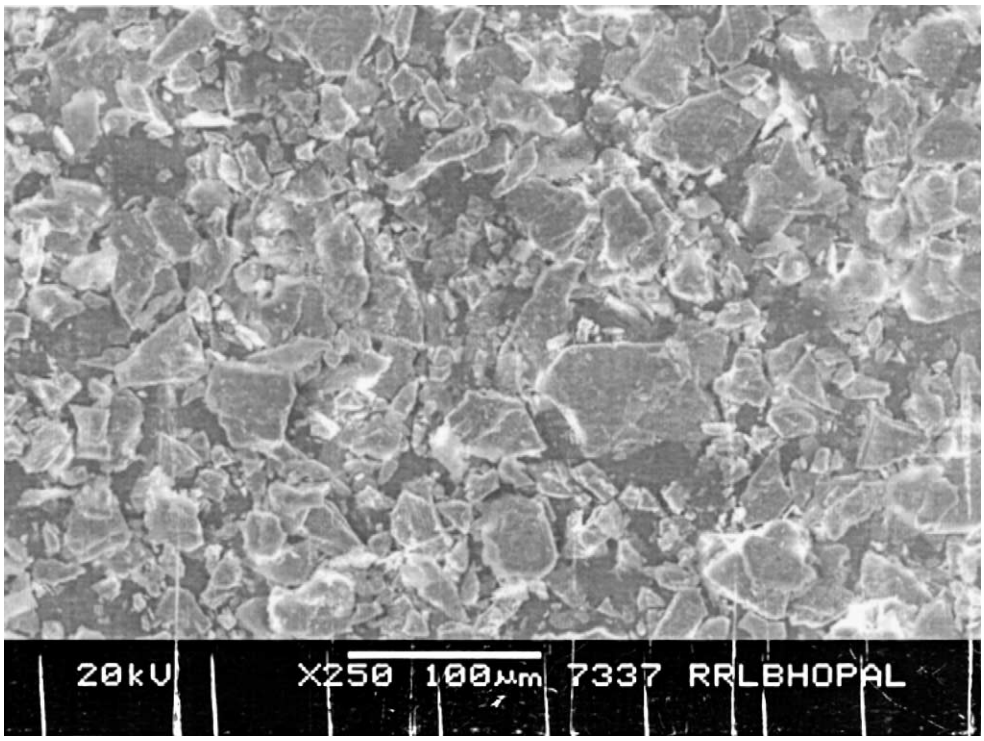

Fig. 7. SEM micrograph of talc with 10% H_3PO_4.

bigger (>25 μm) size corresponding to different phases (cf. Fig. 9).

4. Discussion

To start with, attempts were made to compress talc (in the presence of moisture). However, the green body did not posses sufficient mechanical strength for handling and hence compression of the talc tile with 10% (w/w) plasticizer (starch) was attempted. The green body so formed had sufficient strength required for handling but on sintering at 950 °C for 1 h, the fired body did not posses mechanical strength. Talc has been reported [15] to undergo dehydroxylation reaction forming enstatite and small amounts of silica. The absence of strength in the sintered body indicates that the phases formed on dehydroxylation are not capable of providing mechanical strength to the fired body. A

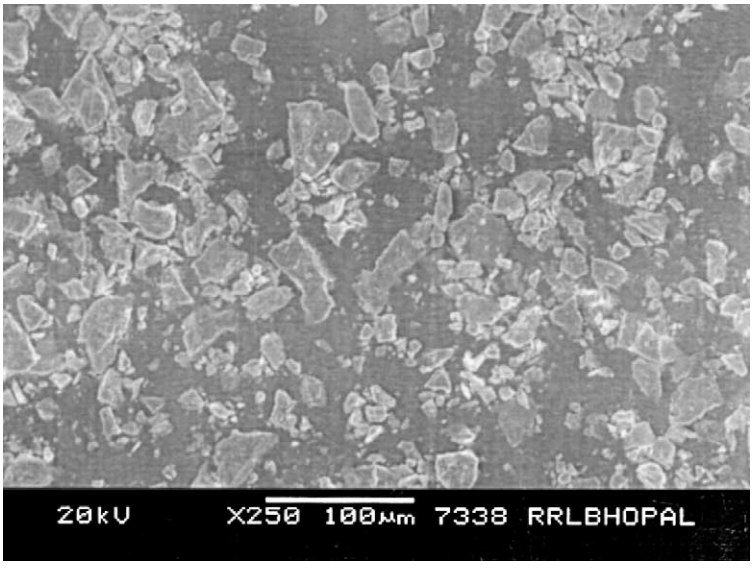

Fig. 8. SEM micrograph of talc with 10% H_3PO_4 and 10% Na_2CO_3.

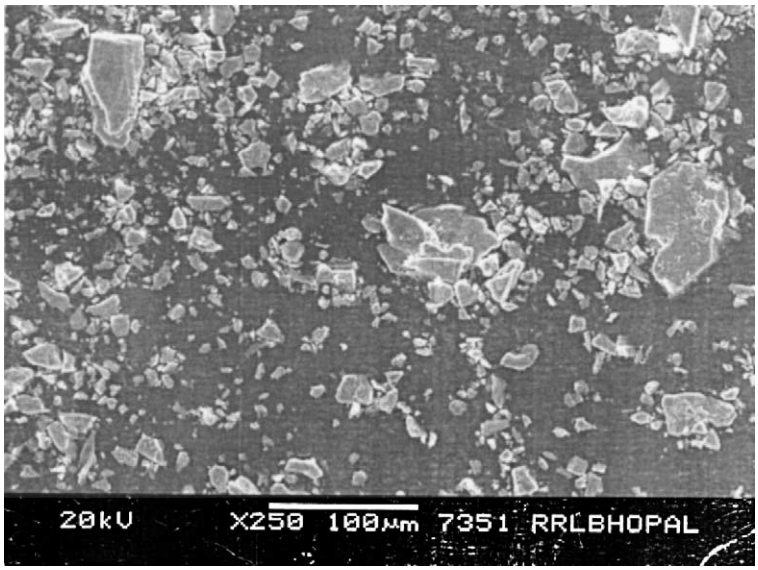

Fig. 9. SEM micrograph of talc with 10% SHMP.

comparison of the SEM micrographs of talc with and without heat treatment (cf. Figs. 5 and 6) shows that while some flakes of talc are still present due to incomplete dehydroxylation, a large number of smaller crystals of irregular shape are observed to be formed on heat treatment at 950 °C.

On addition of 10% sodium carbonate to talc, the sintered body is observed to possess mechanical strength (impact strength 2.96 J/m^2), which may be attributed to the formation of additional new phases, viz. $Na_2Si_2O_5$ and Na_2MgSiO_4. The observation of significant percentage of small particles in the SEM (cf. Fig. 10) of the sintered powder indicates brittleness of the phase(s). Further, a comparison of SEM micrographs of heat-treated talc and sintered talc + Na_2CO_3 composition shows the absence of remainder talc flakes in the latter indicating the role of Na_2CO_3 as an activator in the completion of dehydroxylation reaction. The absence of peaks due to silica in X-ray diffraction studies is attributable to its utilization in the formation of $Na_2Si_2O_5$ and

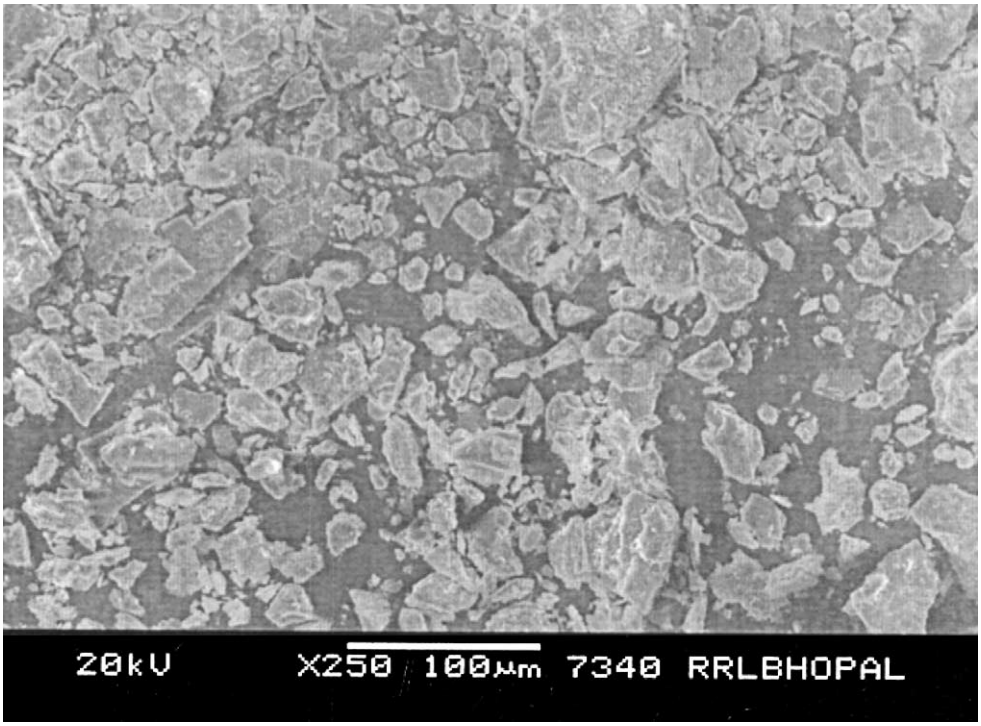

Fig. 10. SEM micrograph of talc with 10% Na_2CO_3.

Na_2MgSiO_4 due to the presence of significant amount of sodium (4.33 g from Na_2CO_3 + 0.80 g from talc).

On sintering of talc with 10% phosphoric acid, the $Mg(PO_3)_2$ and $Mg_3(PO_4)_2$ formed by reaction between phosphoric acid and dehydroxylated talc appear to be responsible for the observation of significantly high impact strength (4.54 J/m^2). It is notable that talc mineral contains very little alkali metal ions and hence the $Na_2Si_2O_5$ and Na_2MgSiO_4 phases are observed to be absent in this case. Further, the phosphate ions are observed to be an activator for dehydroxylation and silica formation from talc as evidenced from the presence of silica in the X-ray diffractograms. The SEM micrographs (cf. Fig. 7) show that as compared to talc + 10% Na_2CO_3 composition (cf. Fig. 10), the content of small size crystals is significantly lower in the sintered talc + 10% H_3PO_4 composition and hence it is inferred that the $Mg(PO_3)_2$ and $Mg_3(PO_4)_2$ phases are less brittle as compared to $Na_2Si_2O_5$ and Na_2MgSiO_4 phases. The higher impact strength of ceramic samples made from talc + 10% H_3PO_4 composition (4.54 J/m^2) as compared to that of those made from talc + 10% Na_2CO_3 (2.96 J/m^2) further corroborates this inference.

When both 10% Na_2CO_3 + 10% H_3PO_4 are added to the talc, the X-ray diffractograms show the peaks corresponding to $Na_2Si_2O_5$, $Mg(PO_3)_2$, and a new phosphatic phase $NaMgPO_4$ while the peak corresponding to $Mg_3(PO_4)_2$ phase is absent. This may be attributed to the availability of significant quantity of sodium ions, which facilitates formation of $NaMgPO_4$ and Na_2MgSiO_4, at the expense of magnesium-rich $Mg_3(PO_4)_2$ phase. The observation of high impact strength (4.53 J/m^2) in this composition may be attributed to the $Mg(PO_3)_2$, and possibly, $NaMgPO_4$ phases. The significantly large size crystals observed in the SEM micrograph of talc + 10% H_3PO_4 composition (cf. Fig. 7) are also observed to be absent in the micrograph of talc + 10% Na_2CO_3 + 10% H_3PO_4 composition (cf. Fig. 8). It is likely that the large size crystals in Fig. 7 correspond to $Mg_3(PO_4)_2$ phase.

In the cases of sintering of talc with 7, 8, 9 or 10% SHMP, Na_2MgSiO_4, $Na_2Si_2O_5$ and $NaMgPO_4$ are formed which may be responsible for the observed mechanical strength of the sintered bodies. Further, in all the four compositions containing SHMP, the peaks corresponding to silica, whose intensity increases with SHMP content, are observed. This indicates the role of SHMP as an activator for dehydroxylation and lowering the temperatures of transformations during sintering. In the composition containing 10% SHMP, the quantity of sodium is only 3.05 g (2.25 g from SHMP and 0.80 g from talc) and hence the silica formed is not fully utilized in forming $Na_2Si_2O_5$ and Na_2MgSiO_4 phases, as was the case when 10% Na_2CO_3 was used.

The formation of $Mg_3(PO_4)_2$/$Mg(PO_3)_2$ was observed when 10% H_3PO_4 was used (with or without 10% Na_2CO_3). However, these phases are absent in sintered talc + SHMP compositions. This may be attributed to the fact that 10% H_3PO_4 provides 9.6 g, whereas 10% SHMP provides only 7.75 g phosphate and hence the formation of phosphate-rich $Mg_3(PO_4)_2$ and $Mg(PO_3)_2$ phases is suppressed in the latter case. The improvement in impact strength with increasing SHMP content may be attributed to the observed increase in the content of $NaMgPO_4$. The improvement in the impact strength with increasing SHMP content, in spite of decrease in the contents of $Na_2Si_2O_5$ and Na_2MgSiO_4 in the fired tiles reaffirms that the phosphatic phase is more effective in providing mechanical strength.

The SEM micrograph of sintered talc + 10% SHMP composition (cf. Fig. 9) shows the material to contain a mix of small size (5–10 μm) and bigger crystals (>25 μm). The small size crystals may possibly correspond to brittle $Na_2Si_2O_5$, phase while $NaMgPO_4$ may be present in the form of observed bigger crystals.

5. Conclusions

Based on the above results, following conclusions can be drawn:

1. Sodium carbonate, phosphoric acid and SHMP, all the three act as activators of sintering and on a weight/weight basis, their effectiveness is in the order H_3PO_4 > SHMP > Na_2CO_3.
2. The impact strength of the talc-based sintered tiles increases with increase in SHMP content in 7–10% (w/w) range.
3. The magnesium phosphate crystals formed during sintering of talc – 10% H_3PO_4 are of larger size and less brittle as compared to crystals formed in other compositions.

Acknowledgements

The authors are thankful to Dr. N. Ramakrishnan, Director, RRL (Bhopal), for his keen interest in the work, to Dr. S. Das for X-ray diffraction measurements and to Shri Mulayam Singh Yadav and T.S.V. Chakradhar Rao for SEM studies.

References

[1] C.A. Sorrell, G.F. Sandstorm, in: H.S. Zim (Ed.), The Rocks & Minerals of the World, Collins St. James Place, London, 1980, p. 192.
[2] S.W. Bailey, in: G.W. Brindley, G. Brown (Eds.), Crystal Structure of Clay Minerals & Their X-ray Identification, Mineralogical Society, London, 1980, pp. 39–40.
[3] M. Grayson (Executive Ed.), KIRK-OTHMER: Encyclopedia of Chemical Technology, Wiley, vol. 22, 1983, pp. 523–526.
[4] Indian Mineral Year Book, Indian Bureau of Mines, Ministry of Mines, Nagpur, 1996, pp. 590–597.
[5] P. Harris, Global talc review, Ind. Miner. 406 (2001) 39–45.
[6] R.L. Johnson, Annual minerals review, talc, Am. Ceram. Soc. Bull. 79 (8) (2000) 79–81.
[7] Luzenac mineral talc from web site www.Luzenac.com

[8] S.K. Mukherji, R.M. Savani, B.B. Mochhoya, Talc its ceramic significance, Indian Ceram. 28 (12) (1986) 256–261.
[9] Yu. Yantang, M. Luping, Substituting talc, Ind. Miner. 389 (2000) 47–51.
[10] A.I. Vogel, A Text Book of Quantitative Inorganic Analysis, ELBS, London, 1984.
[11] Mineral Powder Diffraction File Search Manual, JCPDS International Center for Diffraction Data, Swarthmare, USA, 1980.
[12] IS No. 777 Indian Standard Specification of Glazed Earthenware Tiles, 1970.
[13] S.S. Amritphale, N. Chandra, Low temperature sintering pyrophyllite compositions for wall tiles, J. Can. Ceram. Soc. 64 (4) (1995) 241–244.
[14] S. Bhasin, S.S. Amritphale, N. Chandra, Effect of addition of pyrophyllite on the sintering characteristics of fly ash based ceramic wall tiles, Br. Ceram. Trans. 102 (2) (2003) 1–4.
[15] H.D. Santos, K. Yada, Thermal transformation of talc as studied by electron optical methods, Clays Clay Miner. 36 (4) (1988) 289–297.
[16] A. Gupta, New alumino silicate minerals for composite and ceramic product, Ph.D. thesis, Barkatullah University, Bhopal, India, 1988, p. 58.
[17] S.S. Amritphale, N. Chandra, Thermal transformation of pyrophyllite mineral: effect of a complex activator of sintering, Silicate Ind. 62 (11/12) (1997) 205–209.
[18] S.S. Amritphale, N. Chandra, R. Kumar, Sintering behaviour of pyrophyllite mineral: effect of some alkali and alkaline earth metal carbonates, J. Mater. Sci. 27 (1992) 4797–4804.
[19] S.S. Amritphale, N. Chandra, S. Bhasin, Optimisation of processing parameters for making pyrophyllite based ceramic tiles using di-sodium hydrogen phosphate binder, Br. Ceram. Trans. 100 (2001) 279–283.